

# LEARNING PERCEPTUAL REPRESENTATIONS FOR GAMING NR-VQA WITH MULTI-TASK FR SIGNALS

Yu-Chih Chen<sup>1,2</sup>, Michael Wang<sup>1</sup>, Chieh-Dun Wen<sup>1</sup>, Kai-Siang Ma<sup>1</sup>, Avinab Saha<sup>2†</sup>, Li-Heng Chen<sup>2,3</sup>, Alan Bovik<sup>2</sup>

<sup>1</sup>National Yang Ming Chiao Tung University, <sup>2</sup>The University of Texas at Austin, <sup>3</sup>Netflix Inc.

†Work done at UT Austin; Avinab Saha is now at Google Research.

## ABSTRACT

No-reference video quality assessment (NR-VQA) for gaming videos is challenging due to limited human-rated datasets and unique content characteristics including fast motion, stylized graphics, and compression artifacts. We present MTL-VQA, a multi-task learning framework that uses full-reference metrics as supervisory signals to learn perceptually meaningful features without human labels for pretraining. By jointly optimizing multiple full-reference (FR) objectives with adaptive task weighting, our approach learns shared representations that transfer effectively to NR-VQA. Experiments on gaming video datasets show MTL-VQA achieves performance competitive with state-of-the-art NR-VQA methods across both MOS-supervised and label-efficient/self-supervised settings.

**Index Terms**— Video Quality Assessment (VQA), No-reference VQA, Multitask learning

## 1. INTRODUCTION

Cloud gaming has grown rapidly with high-bandwidth wireless networks and modern mobile devices. Unlike natural videos, gaming content is computer-generated and exhibits distinctive statistics—including fast motion, stylized graphics, user-interface overlays (HUD), and codec-induced artifacts—that violate assumptions commonly exploited by natural-scene-based image quality assessment (IQA)/video quality assessment (VQA) models. In the cloud gaming setting, reference videos are not accessible on the client side; hence no-reference (NR) VQA is required at inference to monitor quality of experience under bitrate, latency, and computational constraints. However, NR VQA is intrinsically more challenging than full-reference (FR) VQA: in the absence of a reference signal, the predictor must infer perceived quality directly from entangled content–distortion statistics, which imposes tighter identifiability and statistical limits. In general, NR methods underperform strong FR baselines when trained under comparable data and compute budgets.

Despite growing practical demand, existing gaming VQA datasets (LIVE-YouTube Gaming [1], LIVE-Meta MCG [2], YouTube UGC-Gaming only [3]) remain relatively small and

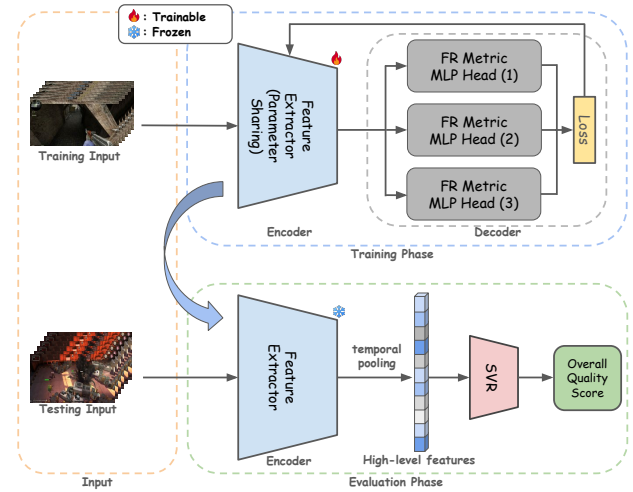


**Fig. 1:** MTL-VQA overview. A shared encoder is supervised by multiple FR objectives during training phase, then frozen for NR evaluation with a lightweight SVR head on temporally pooled features. Training/evaluation specifics are detailed in Sec. 3.1–3.2.

sparsely labeled, limiting fully supervised deep learning-based NR models. To mitigate annotation scarcity, prior works [4, 5, 6, 7] have proposed to train NR predictors using a single FR proxy, e.g., Video Multimethod Assessment Fusion (VMAF) [8], as supervision. While effective to a degree, this strategy ties the learned representation to one specific proxy, introducing label bias and limiting generalization across domains—for example, from professionally generated content (PGC) to user-generated content (UGC) and across heterogeneous distortions and game genres.

We address these limitations with MTL-VQA, a multi-task framework that leverages multiple FR metrics as complementary supervisory signals to learn frame-level perceptual representations without human labels for pretraining on gaming videos. Instead of relying on a single proxy, we treat several FR metrics as distinct tasks and optimize them jointly using a gradient-balancing strategy based on the Multiple Gradient Descent Algorithm (MGDA) / MinNormSolver [9]. After proxy-supervised pretraining on PGC, we freeze the backbone and train only a support vector regressor (SVR) on features obtained via temporal pooling, enabling label-efficient

adaptation to NR-VQA on new gaming datasets.

Our contributions are summarized as follows:

- **Label efficiency for gaming NR-VQA under domain shift.** We show that the MTL-pretrained backbone enables strong few-shot calibration to human MOS under PGC-to-UGC shifts. With Ridge adaptation on as few as  $K=50$  labeled clips, MTL-VQA yields substantial gains over zero-shot transfer, and with  $K=100$  it reaches a PLCC of **0.9301** on YouTube UGC-Gaming. These results indicate that the learned representation transfers robustly across datasets and remains effective under gaming-specific distribution shifts such as HUD overlays and stylized rendering.
- **Multi-proxy FR supervision with principled gradient balancing.** We propose MTL-VQA, a multi-task pretraining framework that learns a quality-aware representation from multiple complementary FR metrics using MGDA/MinNormSolver to mitigate proxy-specific dominance. This multi-proxy training improves the performance-label trade-off compared to single-proxy pretraining and fixed-weight multi-loss baselines.
- **Practical and reference-free deployment for cloud gaming.** At test time, our approach is fully no-reference and adds only a lightweight regressor on temporally sampled and pooled features from a standard ResNet-50 backbone, enabling efficient real-time quality monitoring in cloud gaming systems. Code and pretrained models will be released.

## 2. RELATED WORK

### 2.1. FR VQA Models

FR IQA/VQA compares a distorted signal with its pristine reference. While classic measures (e.g., PSNR, SSIM [10], MS-SSIM [11]) are widely used, learned fusion metrics such as VMAF [8] often better align with perceptual quality and have shown strong correlation with MOS in gaming streaming scenarios [12, 13]. In cloud gaming, references are unavailable at inference, making FR metrics valuable as proxy supervisory signals for learning quality-aware representations and training deployable no-reference predictors.

### 2.2. NR VQA Models for Gaming Videos

Most NR VQA methods were developed under natural-scene statistics and trained on natural content [14, 15, 16]. Gaming videos are computer-generated and contain synthetic textures, HUD overlays, and distinct motion patterns, leading to distribution shift and degraded performance of conventional

NR models. Consequently, several gaming-oriented NR approaches have been proposed [4, 5, 6], with recent deep models leveraging higher-level semantics [7, 17]. However, existing methods remain limited by scarce MOS labels and reliance on a single proxy objective, motivating multi-objective (MTL) proxy supervision to reduce proxy-specific bias and improve adaptation with limited MOS.

## 3. METHOD

As illustrated in Fig. 1, our approach first learns a shared representation by supervising a trainable encoder with multiple FR objectives on PGC datasets. At evaluation time, the encoder is frozen and a lightweight regressor produces NR quality predictions on target clips. We defer training and evaluation details to the subsequent subsections.

### 3.1. Problem Setup and Data

We consider gaming VQA under two operational regimes. PGC denotes controlled pipelines (e.g., cloud streaming with known encoder settings), where a pristine reference is available server-side and FR metrics can be computed on paired (reference, distorted) stimuli. UGC denotes end-user recordings and platform transcodes with heterogeneous, composite degradations; references are unavailable and human annotations are typically scarce.

**Dataset-disjoint Training/Evaluation.** Training–test partitions are dataset-disjoint by design: FR proxy supervision is derived exclusively from PGC datasets {GamingVideoSET, KUGVD, CGVDS} (training phase in Fig. 1), whereas NR evaluation is conducted on separate corpora—LIVE-Meta MCG (PGC) and YouTube UGC-Gaming only / LIVE-YouTube Gaming (UGC) (evaluation phase in Fig. 1). This eliminates leakage and directly measures cross-dataset transfer.

**Proxy Target Generation (PGC).** Instead of relying only on the original reference–distorted pairs bundled in the PGC databases, we generate additional distorted streams by compressing the pristine references with `ffmpeg` under controlled bitrate ladders. Concretely, for each reference clip we encode at 0.25, 0.5, 1, 2, and 5 Mbps (other encoder parameters fixed), producing  $(x, y)$  pairs at scale and enabling abundant frame supervision beyond the original database size. Full-reference targets  $y_i^{(t)} = \text{FR}_t(x_i, y_i)$  including SSIM, MS-SSIM, VMAF, and FovVideoVDP [18] are then computed between each compressed stream  $x_i$  and its pristine  $y_i$ . Note that clip-level targets use  $y^{(t)} = \frac{1}{N} \sum_i y_i^{(t)}$  when required. This procedure preserves the dataset-disjoint split (sources remain PGC) while providing rich, controllable distortions for multi-FR proxy supervision. In total, we obtain 885,000 training frames for proxy supervision.

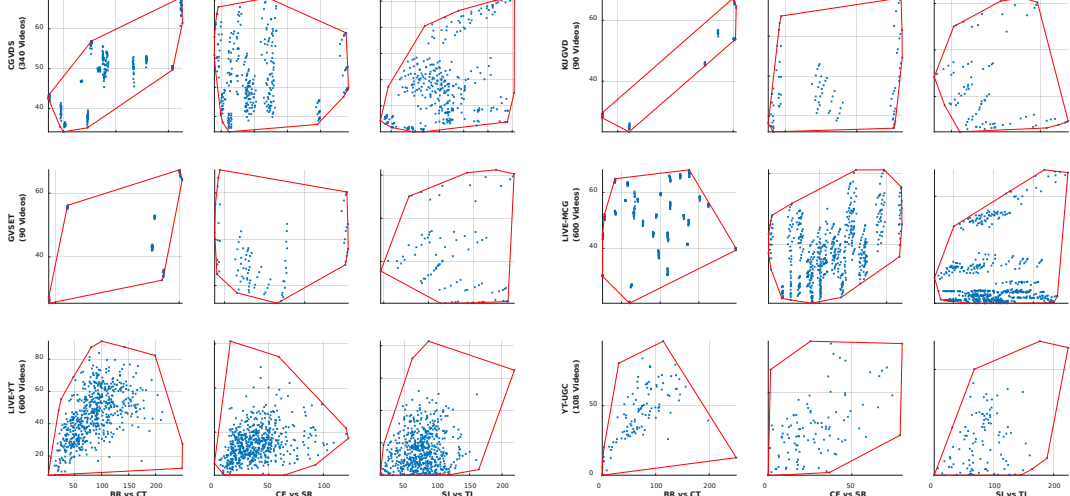


Fig. 2: Source content (blue ‘x’) distribution in paired feature space with corresponding convex hulls (orange boundaries)

### 3.2. Task Formulation and Optimization

Let  $X = \{x_i\}_{i=1}^N$  and  $Y = \{y_i\}_{i=1}^N$  be distorted/reference frames. A shared encoder  $f_{\theta^{\text{sh}}}$  yields  $z_i = f_{\theta^{\text{sh}}}(x_i)$ , and  $\bar{z} = \text{Pool}(\{z_i\})$  is a clip-level representation.

**Multi-task FR Supervision.** Each FR task  $t$  attaches a lightweight head  $h_{\theta^{(t)}}$  (the per-task Multilayer Perceptron [MLP] heads in Fig. 1) to predict  $\hat{y}_i^{(t)}$  from  $z_i$ . We minimize per-task regression losses over frames (or their clip average):

$$\mathcal{L}_t(\theta^{\text{sh}}, \theta^{(t)}) = \frac{1}{N} \sum_{i=1}^N \phi(\hat{y}_i^{(t)}, y_i^{(t)}), \quad (1)$$

$$\hat{y}_i^{(t)} = h_{\theta^{(t)}}(z_i), \quad y_i^{(t)} = \text{FR}_t(x_i, y_i).$$

**Per-task Regression Losses.** We use Smooth- $L_1$  loss as our loss function. Let  $r = \hat{y}^{(t)} - y^{(t)}$ . The Smooth- $L_1$  loss with parameter  $\beta$  is

$$\phi_{\text{smooth-}L_1}(r; \beta) = \begin{cases} \frac{r^2}{2\beta}, & |r| < \beta, \\ |r| - \frac{\beta}{2}, & \text{otherwise,} \end{cases} \quad \text{with } \beta = 1. \quad (2)$$

**Adaptive Task Weighting via MinNormSolver.** To mitigate gradient interference on the shared encoder parameters  $\theta^{\text{sh}}$ , we compute a convex combination of encoder gradients only. For each mini-batch, we first backpropagate each  $\mathcal{L}_t$  separately to obtain  $g_t^{\text{enc}} = \nabla_{\theta^{\text{sh}}} \mathcal{L}_t(\theta^{\text{sh}}, \theta^{(t)})$ . We then solve

$$\alpha^* = \arg \min_{\alpha \succeq 0, \|\alpha\|_1=1} \left\| \sum_{t=1}^T \alpha_t g_t^{\text{enc}} \right\|_2^2,$$

via the geometric MinNormSolver, and form a joint loss  $\mathcal{L}_{\text{joint}} = \sum_{t=1}^T \alpha_t^* \mathcal{L}_t$  for the second forward/backward pass to update both  $\theta^{\text{sh}}$  and  $\{\theta^{(t)}\}$ .

| METHODS     | GAMINGVIDESET |               |               | KUGVD         |               |               | CGVDS         |               |               |
|-------------|---------------|---------------|---------------|---------------|---------------|---------------|---------------|---------------|---------------|
|             | SRCC↑         | PLCC↑         | RMSE↓         | SRCC↑         | PLCC↑         | RMSE↓         | SRCC↑         | PLCC↑         | RMSE↓         |
| PSNR        | 0.8086        | 0.8538        | 0.3959        | 0.8851        | 0.8883        | 0.3747        | 0.7301        | 0.7424        | 0.5138        |
| SSIM        | <b>0.9451</b> | <b>0.9629</b> | <b>0.2214</b> | <b>0.9603</b> | <b>0.9659</b> | <b>0.2097</b> | 0.7899        | 0.7918        | 0.4741        |
| MS-SSIM     | 0.9232        | 0.9373        | <b>0.2570</b> | 0.9541        | 0.9660        | 0.2104        | <b>0.8325</b> | <b>0.8310</b> | <b>0.4307</b> |
| VMAF        | 0.8524        | 0.8751        | 0.3953        | <b>0.9028</b> | 0.9172        | <b>0.3509</b> | <b>0.8894</b> | <b>0.8969</b> | <b>0.3417</b> |
| DLM         | <b>0.9365</b> | <b>0.9571</b> | <b>0.2929</b> | 0.6591        | 0.6199        | 0.9517        | 0.6569        | 0.6298        | 0.5975        |
| VIF         | 0.9248        | <b>0.9462</b> | 0.3270        | 0.6342        | 0.5933        | 0.9763        | 0.6516        | 0.6153        | 0.6064        |
| FovVideoVDP | <b>0.9287</b> | 0.9425        | 0.3379        | 0.7114        | 0.7119        | 0.8518        | 0.5255        | 0.5729        | 0.6304        |
| LPIPS       | 0.7945        | 0.8092        | 0.5272        | 0.8327        | 0.8405        | 0.5610        | 0.6454        | 0.6632        | 0.5929        |
| DISTS       | 0.7977        | 0.8088        | 0.5276        | 0.8532        | 0.8628        | 0.5234        | <b>0.8239</b> | <b>0.8398</b> | <b>0.4301</b> |

Table 1: FR IQA/VQA metrics performance on training datasets (GamingVideoSET, KUGVD, and CGVDS).

### 3.3. Domain-Gap Considerations

Gaming VQA faces distribution shifts between: (i) PGC training and UGC evaluation, (ii) FR-proxy supervision and NRMOS prediction, and (iii) stylized rendering, HUD overlays, and bitrate variations. As shown in Fig. 2, distortions in PGC follow predictable patterns imposed by controlled degradation rules, whereas UGC displays far more stochastic and irregular behavior in its distribution. We also employ multiple complementary FR proxies and evaluate zero-/few-shot transfer to regularize against these shifts.

### 3.4. Architecture and Implementation

Our pipeline comprises a ResNet-50 encoder  $f_{\theta}(\cdot)$  (ImageNet-initialized), temporal pooling, and a lightweight regressor. Given a clip  $X = \{x_i\}_{i=1}^N$ , we extract frame embeddings  $z_i = f_{\theta}(x_i)$  and aggregate via mean pooling to obtain  $\bar{z} = \text{Pool}(\{z_i\}_{i=1}^N)$ . During FR pretraining, task-specific MLP heads predict FR targets from the shared representation. At evaluation, the encoder is frozen and an SVR maps  $\bar{z}$  to quality score  $\hat{q} = \text{SVR}(\bar{z})$ , avoiding human annotations for pretraining / representation learning. Frames are downsampled (one per two) and resized to  $960 \times 540$ . Training uses SGD with batch size 20.

### 3.5. Multi-Task FR Supervision and Rationale

We select FR objectives by their empirical MOS alignment on PGC datasets (Table 1). Structure-focused metrics (SSIM/MS-SSIM) align best on GamingVideoSET/KUGVD, while VMAF is strongest on CGVDS. To mitigate proxy-specific bias, we combine top FR signals via multi-task learning with adaptive weighting (Sec. 3.2).

## 4. EXPERIMENTS

### 4.1. Experimental Setup

**Datasets and Disjoint Training/Evaluation.** As detailed in Sec. 3.1, FR proxy supervision is derived only from PGC datasets {GamingVideoSET, KUGVD, CGVDS}, while NR evaluation is conducted on different corpora-LIVE-Meta MCG (PGC) and two UGC testbeds (YouTube UGC-Gaming only subset and LIVE-YouTube Gaming). This dataset-disjoint design prevents leakage and directly measures cross-dataset transfer.

For inference on the test sets, we uniformly sample 1 frame per second from each clip. Frames from LIVE-Meta MCG are resized to the dataset’s display-provided height and width, while all other evaluation datasets are resized to  $960 \times 540$  prior to feature extraction.

**Evaluation Protocols.** We consider three protocols on each evaluation set: (i) **Zero-shot (target-label-free; head trained on source MOS only):** freeze the FR-pretrained encoder and train a lightweight MLP head on *source* PGC datasets using their MOS labels; then freeze this head and directly apply the encoder+head to the *target* test set (no target labels). (ii) **Few-shot:** freeze the encoder and fit an RBF-kernel SVR or a Ridge regressor on  $K \in \{10, 20, 50, 100\}$  labeled clips from the target dataset; evaluate on the remaining clips (Table 4). (iii) **Standard split:** For each evaluation dataset, we run 100 independent content-disjoint splits with an 80%/20% train/test ratio. The 80% training portion is further partitioned by content into five folds for cross-validation. SVR hyperparameters ( $C, \gamma$ ) are selected via grid search on the training/validation folds, after which the SVR is retrained on the full training split and evaluated on the held-out 20%. All supervised baselines and our head training follow the same split protocol.

**Evaluation Metrics.** We report rank and linear agreement with MOS using SRCC, KRCC, PLCC, and RMSE. Following common practice and our code path, SRCC/KRCC are computed on *raw* predictions, while PLCC/RMSE are computed *after* applying a logistic mapping. Unless noted, we aggregate results over repeated content-disjoint 80/20 hold-outs and report the *median* across runs. For few-shot experiments, we additionally report medians over 100 random  $K$ -samplings.

### 4.2. Main Results

**Baselines and Results.** We compare MTL-VQA with (i) opinion-unaware handcrafted NR-IQA/VQA baselines, including NIQE and classical feature-based methods such as BRISQUE, TLVQM [19], and VIDEVAL [20]; (ii) opinion-aware supervised learning-based NR-VQA models trained with human subjective scores (MOS/DMOS), including RAPIQUE [16], GAME-VQP [21], VSFA [22], GAMIVAL, FasterVQA [23], and DOVER++ [24]; (iii) self-supervised (unsupervised) representation learning approaches that learn quality-aware features without using human labels for pre-training, including CONTRIQUE [25], ReIQA [26], CONVIQT [27], and CLIP-IQA+ [28]; and (iv) proxy-supervised combined with fine-tuning approaches that first learn from FR metric targets and optionally adapt with MOS labels (e.g., NDNet-Gaming [7]).

As shown in Table 2, MTL-VQA achieves competitive performance across all benchmarks. On LIVE-Meta MCG, it reaches 0.9434 SRCC, comparable to the best-performing baseline (GAMIVAL at 0.9439). On the more challenging YouTube UGC-Gaming testbed, MTL-VQA attains 0.8292 SRCC and surpasses strong learned baselines such as CONVIQT and DOVER++. Notably, contrastive-learning-based NR models (e.g., CONTRIQUE and CONVIQT) also perform strongly, indicating that representation learning is crucial for gaming NR-VQA under label scarcity. In comparison, our gains are achieved with multi-FR proxy supervision on PGC and a frozen backbone with a lightweight SVR head at inference, suggesting better transfer to UGC without relying on extensive MOS-labeled training.

**Few-shot Adaptation.** Table 4 evaluates the label efficiency of our MTL-pretrained representations. While cross-dataset transfer without target supervision remains challenging under large domain shifts, the learned features provide a strong perceptual prior that can be aligned with MOS using only a small number of labeled clips. In the extreme low-data regime (e.g.,  $K=10$ ), Ridge regression is noticeably more stable than SVR, avoiding the numerical instability observed for SVR (e.g., undefined PLCC). On YouTube UGC, Ridge attains a PLCC of 0.7370 when the regressor is transferred across datasets ( $K=0$ ) and reaches 0.9301 with only 100 labeled samples. Overall, these results highlight that multi-task FR pretraining yields transferable representations that support reliable, label-efficient calibration, which is particularly attractive for practical cloud-gaming QoE monitoring where MOS labels are scarce.

### 4.3. Ablation Studies

To quantify the benefit of additional proxy tasks, we compare a single-proxy baseline (ST; VMAF-only) with our multi-proxy pretraining (MTL; VMAF+MS-SSIM+SSIM). As shown in Table 3, MTL improves correlation consistently across all benchmarks, with an average gain of +0.054 SRCC

| DATASET        | LIVE-Meta MCG<br>(600 videos) |               |               |               | LIVE-YouTube Gaming<br>(600 videos) |               |               |               | YouTube UGC-Gaming only<br>(108 videos) |               |               |               |
|----------------|-------------------------------|---------------|---------------|---------------|-------------------------------------|---------------|---------------|---------------|---|---------------|---------------|---------------|
|                | Methods                       | SRCC↑         | KRCC↑         | PLCC↑         | RMSE↓                               | SRCC↑         | KRCC↑         | PLCC↑         | RMSE↓                                   | SRCC↑         | KRCC↑         | PLCC↑         |
| NIQE           | -0.3900                       | -0.2795       | 0.4581        | 16.5475       | 0.2801*                             | N/A           | 0.3037*       | 16.208*       | -0.5512                                 | -0.3889       | 0.5732        | 0.5184        |
| BRISQUE        | 0.7153                        | 0.5278        | 0.7206        | 12.6254       | 0.6037*                             | N/A           | 0.6383*       | 16.208*       | 0.3357                                  | 0.2364        | 0.4588        | 0.5673        |
| TLVQM          | 0.6553                        | 0.4777        | 0.6889        | 13.5413       | 0.7484*                             | N/A           | 0.7564*       | 11.134*       | 0.6885                                  | 0.5031        | 0.7267        | 0.4433        |
| VIDEVAL        | 0.7601                        | 0.5754        | 0.7741        | 12.0348       | 0.8071*                             | N/A           | 0.9119*       | 10.093*       | 0.6736                                  | 0.4978        | 0.7199        | 0.4022        |
| RAPIQUE        | 0.8768                        | 0.7015        | 0.9043        | 8.0669        | 0.8028*                             | N/A           | 0.8248*       | 9.661*        | 0.6828                                  | 0.5034        | 0.7399        | 0.4339        |
| GAME-VQP       | 0.8773                        | 0.6915        | 0.8954        | 8.3778        | <b>0.8563*</b>                      | N/A           | 0.8754*       | 8.533*        | N/A                                     | N/A           | N/A           | N/A           |
| NDNet-Gaming   | 0.8506                        | 0.6619        | 0.8401        | 9.9466        | 0.4562*                             | N/A           | 0.4690*       | 14.941*       | 0.2726                                  | 0.1871        | 0.3747        | 0.5866        |
| VSFA           | 0.9143                        | 0.7485        | 0.9259        | 7.1455        | 0.7762*                             | N/A           | 0.8014*       | 10.396*       | 0.6872                                  | 0.5152        | 0.7103        | 0.4806        |
| GAMIVAL        | <b>0.9439</b>                 | <b>0.7962</b> | <b>0.9526</b> | <b>5.6941</b> | 0.8111                              | N/A           | 0.8321        | 9.2995        | <b>0.7277</b>                           | <b>0.5441</b> | <b>0.7640</b> | 0.4320        |
| CONTRIQUE      | 0.9310                        | 0.7768        | 0.9378        | 6.3556        | <b>0.8556</b>                       | <b>0.6738</b> | <b>0.8791</b> | <b>8.0262</b> | 0.7059                                  | 0.5306        | 0.7475        | <b>0.3889</b> |
| ReIQA          | 0.7557                        | 0.5669        | 0.7681        | 11.7441       | 0.3730                              | 0.2609        | 0.3912        | 15.5303       | 0.5780                                  | 0.4163        | 0.7044        | 0.4165        |
| CONVIQT        | <b>0.9364</b>                 | <b>0.7835</b> | <b>0.9423</b> | <b>6.1939</b> | <b>0.8609</b>                       | <b>0.6806</b> | <b>0.8850</b> | <b>7.8534</b> | <b>0.7535</b>                           | <b>0.5785</b> | <b>0.7894</b> | <b>0.3560</b> |
| CLIP-IQA+      | 0.6998                        | 0.4969        | 0.7268        | 12.3443       | 0.4315                              | 0.2951        | 0.5372        | 14.2693       | 0.6585                                  | 0.4688        | 0.6847        | 0.4611        |
| DOVER++        | 0.7855                        | 0.5850        | 0.8187        | 10.3191       | 0.6530                              | 0.4765        | 0.7258        | 11.6374       | 0.6822                                  | 0.4926        | 0.7084        | 0.4465        |
| FasterVQA      | 0.4415                        | 0.3046        | 0.4770        | 15.7958       | 0.2603                              | 0.1767        | 0.2889        | 16.1962       | 0.2981                                  | 0.2019        | 0.3868        | 0.5834        |
| MTL-VQA [Ours] | <b>0.9434</b>                 | <b>0.7951</b> | <b>0.9506</b> | <b>5.7912</b> | 0.8486                              | <b>0.6681</b> | <b>0.8758</b> | <b>8.1330</b> | <b>0.8292</b>                           | <b>0.6468</b> | <b>0.8643</b> | <b>0.2924</b> |

**Table 2:** Median performance comparison of VQA methods across three gaming video quality databases: LIVE-Meta MCG, LIVE-YouTube Gaming, and YouTube UGC-Gaming only. The results are based on 100 random train/test splits. The underlined and **boldfaced** entries represent the best and top three performers in each column.  $*$  denotes values cited from the authors of GAME-VQP.

| DATASET | LIVE-Meta MCG |               |               |               | LIVE-YouTube Gaming |               |               |               | YouTube UGC-Gaming only |               |               |       |
|---------|---------------|---------------|---------------|---------------|---------------------|---------------|---------------|---------------|-------------------------|---------------|---------------|-------|
|         | Methods       | SRCC↑         | KRCC↑         | PLCC↑         | RMSE↓               | SRCC↑         | PLCC↑         | RMSE↓         | SRCC↑                   | KRCC↑         | PLCC↑         | RMSE↓ |
| ST-VQA  | 0.8965        | 0.7288        | 0.9091        | 7.6649        | 0.8254              | 0.8536        | 8.7593        | 0.7377        | 0.5671                  | 0.7847        | 0.3608        |       |
| MTL-VQA | <b>0.9434</b> | <b>0.7951</b> | <b>0.9506</b> | <b>5.7912</b> | <b>0.8486</b>       | <b>0.8758</b> | <b>8.1330</b> | <b>0.8292</b> | <b>0.6468</b>           | <b>0.8643</b> | <b>0.2924</b> |       |

**Table 3:** Ablation study comparing the performance of Single-Task (ST; VMAF-only) VQA against our proposed Multi-Task Learning (MTL; VMAF+MS-SSIM+SSIM) VQA framework across three gaming databases. The ST baseline only employs the VMAF head, while MTL utilizes multiple quality metrics heads (VMAF, MS-SSIM, SSIM).

| Samples (K) | LIVE-YouTube Gaming |        |        |        | YouTube UGC-Gaming only |        |        |        |
|-------------|---------------------|--------|--------|--------|-------------------------|--------|--------|--------|
|             | SVR                 |        | Ridge  |        | SVR                     |        | Ridge  |        |
|             | SRCC                | PLCC   | SRCC   | PLCC   | SRCC                    | PLCC   | SRCC   | PLCC   |
| K=0         | 0.2399              | 0.2228 | 0.6951 | 0.7328 | -0.1020                 | 0.2821 | 0.6434 | 0.7370 |
| K=10        | 0.2966              | —      | 0.5114 | 0.5741 | 0.3849                  | 0.3850 | 0.5937 | 0.6611 |
| K=20        | 0.5705              | 0.6089 | 0.6132 | 0.6745 | 0.6642                  | 0.6859 | 0.6679 | 0.7273 |
| K=50        | 0.7155              | 0.7478 | 0.7158 | 0.7578 | 0.7588                  | 0.8058 | 0.7449 | 0.8040 |
| K=100       | 0.7716              | 0.7996 | 0.7696 | 0.8036 | 0.7640                  | 0.8867 | 0.7857 | 0.9301 |

**Table 4:** Zero-shot  $K = 0$  and Few-shot  $K \in \{10, 20, 50, 100\}$  performance of the MTL-VQA model on the LIVE-YouTube Gaming and YouTube UGC datasets. For few-shot evaluation, a regressor (SVR or Ridge) is adapted using  $K$  samples from the target dataset and evaluated on the remaining samples. Reported metrics are SRCC ( $\uparrow$ ) and PLCC ( $\uparrow$ ).

and +0.048 PLCC. Notably, these gains are obtained with a frozen backbone and a lightweight SVR regressor trained on temporally pooled 2048-d features, indicating that multi-FR supervision encourages a more robust and transferable perceptual representation than single-proxy supervision, especially under the PGC→UGC domain shift.

## 5. CONCLUSION

We presented MTL-VQA, a label-efficient pretraining framework for gaming NR-VQA that leverages multiple full-reference objectives to learn robust representations. Across gaming benchmarks, a frozen backbone with a lightweight regressor achieves competitive performance, and multi-proxy

supervision improves correlation over single-metric pretraining. Notably, in few-shot settings, Ridge adaptation with up to 100 labeled clips closes most of the gap to standard-split training, suggesting that representation quality, rather than regressor complexity, is the primary driver. Furthermore, from a deployment perspective, MTL-VQA supports practical cloud-gaming QoE monitoring: server-side FR proxy supervision enables a shared encoder that can be reused client-side for low-latency NR inference with minimal calibration. However, limitations remain on extremely low-quality clips where HUD overlays can dominate pooled features. To address this, future work will explore HUD-aware masking, stronger temporal modeling for fast motion and flicker, and codec/artifact-aware auxiliary tasks to further improve robustness under diverse gaming distortions.

## 6. REFERENCES

- [1] Xiangyu Yu, Zhenqiang Ying, Neil Birkbeck, Yilin Wang, Balu Adsumilli, and Alan C Bovik, “Subjective and objective analysis of streamed gaming videos,” *IEEE Transactions on Games*, vol. 16, no. 2, pp. 445–458, 2023.
- [2] Avinab Saha, Yu-Chih Chen, Chase Davis, Bo Qui, Xiaomin Wang, Rahul Gowda, Ioannis Katsavounidis, and Alan C Bovik, “Study of subjective and objective quality assessment of mobile cloud gaming videos,” in *IEEE Transactions on Image Processing*, in peer review.
- [3] Yilin Wang, Sasi Inguva, and Balu Adsumilli, “YouTube

UGC dataset for video compression research,” in *2019 IEEE 21st International Workshop on Multimedia Signal Processing (MMSP)*, 2019, pp. 1–5.

[4] Saman Zadtootaghaj, Nabajeet Barman, Steven Schmidt, Maria G Martini, and Sebastian Möller, “NR-GVQM: A no reference gaming video quality metric,” in *2018 IEEE International Symposium on Multimedia (ISM)*. IEEE, 2018, pp. 131–134.

[5] Steve Göring, Rakesh Rao Ramachandra Rao, and Alexander Raake, “NOFU—a lightweight no-reference pixel based video quality model for gaming content,” in *2019 Eleventh International Conference on Quality of Multimedia Experience (QoMEX)*. IEEE, 2019, pp. 1–6.

[6] Nabajeet Barman, Emmanuel Jammeh, Seyed Ali Ghorashi, and Maria G Martini, “No-reference video quality estimation based on machine learning for passive gaming video streaming applications,” *IEEE Access*, vol. 7, pp. 74511–74527, 2019.

[7] Markus Utke, Saman Zadtootaghaj, Steven Schmidt, Sebastian Bosse, and Sebastian Möller, “NDNetGaming—development of a no-reference deep CNN for gaming video quality prediction,” *Multimedia Tools and Applications*, pp. 1–23, 2020.

[8] Zhi Li, Anne Aaron, Ioannis Katsavounidis, Anush Moorthy, and Megha Manohara, “Toward a practical perceptual video quality metric,” *The Netflix Tech Blog*, vol. 6, no. 2, 2016.

[9] Ozan Sener and Vladlen Koltun, “Multi-task learning as multi-objective optimization,” *Advances in neural information processing systems*, vol. 31, 2018.

[10] Zhou Wang, Alan C Bovik, Hamid R Sheikh, and Eero P Simoncelli, “Image quality assessment: from error visibility to structural similarity,” *IEEE transactions on image processing*, vol. 13, no. 4, pp. 600–612, 2004.

[11] Zhou Wang, Eero P Simoncelli, and Alan C Bovik, “Multi-scale structural similarity for image quality assessment,” in *The thirty-seventh asilomar conference on signals, systems & computers, 2003*. Ieee, 2003, vol. 2, pp. 1398–1402.

[12] Nabajeet Barman, Saman Zadtootaghaj, Steven Schmidt, Maria G Martini, and Sebastian Möller, “An objective and subjective quality assessment study of passive gaming video streaming,” *International Journal of Network Management*, vol. 30, no. 3, pp. e2054, 2020.

[13] Nabajeet Barman, Steven Schmidt, Saman Zadtootaghaj, Maria G Martini, and Sebastian Möller, “An evaluation of video quality assessment metrics for passive gaming video streaming,” in *Proceedings of the 23rd packet video workshop*, 2018, pp. 7–12.

[14] Anish Mittal, Anush Krishna Moorthy, and Alan Conrad Bovik, “No-reference image quality assessment in the spatial domain,” *IEEE Transactions on Image Processing*, vol. 21, no. 12, pp. 4695–4708, 2012.

[15] Anish Mittal, Rajiv Soundararajan, and Alan C Bovik, “Making a “completely blind” image quality analyzer,” *IEEE Signal Processing Letters*, vol. 20, no. 3, pp. 209–212, 2012.

[16] Zhengzhong Tu, Xiangxu Yu, Yilin Wang, Neil Birkbeck, Balu Adsumilli, and Alan C Bovik, “RAPIQUE: Rapid and accurate video quality prediction of user generated content,” *IEEE Open Journal of Signal Processing*, vol. 2, pp. 425–440, 2021.

[17] Yu-Chih Chen, Avinab Saha, Chase Davis, Bo Qiu, Xiaoming Wang, Rahul Gowda, Ioannis Katsavounidis, and Alan C Bovik, “Gamival: video quality prediction on mobile cloud gaming content,” *IEEE Signal Processing Letters*, vol. 30, pp. 324–328, 2023.

[18] Rafał K Mantiuk, Gyorgy Denes, Alexandre Chapiro, Anton Kaplanyan, Gizem Rufo, Romain Bachy, Trisha Lian, and Anjul Patney, “Fovvideovdp: A visible difference predictor for wide field-of-view video,” *ACM Transactions on Graphics (TOG)*, vol. 40, no. 4, pp. 1–19, 2021.

[19] Jari Korhonen, “Two-level approach for no-reference consumer video quality assessment,” *IEEE Transactions on Image Processing*, vol. 28, no. 12, pp. 5923–5938, 2019.

[20] Zhengzhong Tu, Yilin Wang, Neil Birkbeck, Balu Adsumilli, and Alan C Bovik, “UGC-VQA: Benchmarking blind video quality assessment for user generated content,” *IEEE Transactions on Image Processing*, vol. 30, pp. 4449–4464, 2021.

[21] Xiangxu Yu, Zhengzhong Tu, Neil Birkbeck, Yilin Wang, Balu Adsumilli, and Alan C Bovik, “Perceptual quality assessment of ugc gaming videos,” *arXiv preprint arXiv:2204.00128*, 2022.

[22] Dingquan Li, Tingting Jiang, and Ming Jiang, “Quality assessment of in-the-wild videos,” in *Proceedings of the 27th ACM International Conference on Multimedia*, 2019, pp. 2351–2359.

[23] Haoning Wu, Chaofeng Chen, Liang Liao, Jingwen Hou, Wenxiu Sun, Qiong Yan, Jinwei Gu, and Weisi Lin, “Neighbourhood representative sampling for efficient end-to-end video quality assessment,” *IEEE Transactions on Pattern Analysis and Machine Intelligence*, vol. 45, no. 12, pp. 15185–15202, 2023.

[24] Haoning Wu, Erli Zhang, Liang Liao, Chaofeng Chen, Jingwen Hou, Annan Wang, Wenxiu Sun, Qiong Yan, and Weisi Lin, “Exploring video quality assessment on user generated contents from aesthetic and technical perspectives,” in *Proceedings of the IEEE/CVF International Conference on Computer Vision*, 2023, pp. 20144–20154.

[25] Pavan C. Madhusudana, Neil Birkbeck, Yilin Wang, Balu Adsumilli, and Alan C. Bovik, “Image quality assessment using contrastive learning,” *IEEE Transactions on Image Processing*, vol. 31, pp. 4149–4161, 2022.

[26] Avinab Saha, Sandeep Mishra, and Alan C. Bovik, “Re-IQA: Unsupervised learning fo brar h abdulnabi, gang wang, r image quality assessment in the wild,” in *Proceedings of the IEEE/CVF Conference on Computer Vision and Pattern Recognition (CVPR)*, June 2023, pp. 5846–5855.

[27] Pavan C. Madhusudana, Neil Birkbeck, Yilin Wang, Balu Adsumilli, and Alan C. Bovik, “Convigt: Contrastive video quality estimator,” *IEEE Transactions on Image Processing*, vol. 32, pp. 5138–5152, 2023.

[28] Jianyi Wang, Kelvin CK Chan, and Chen Change Loy, “Exploring clip for assessing the look and feel of images,” in *AAAI*, 2023.